chemosensors

Article

Evaluating the Intensity of Bitter–Astringent Interactive Perception in Green Tea Based on the Weber–Fechner Law

Siying Li [1,2], Dongdong Du [1,2], Shaoming Cheng [1] and Zhenbo Wei [1,2,*]

[1] Department of Biosystems Engineering, Zhejiang University, 866 Yuhangtang Road, Hangzhou 310058, China; lisiying@zju.edu.cn (S.L.); dudd@zju.edu.cn (D.D.); chengshaoming@zju.edu.cn (S.C.)
[2] Zhejiang Key Laboratory of Intelligent Sensing and Robotics for Agriculture, Department of Biosystems Engineering and Food Science, Zhejiang University, Hangzhou 310058, China
* Correspondence: weizhb@zju.edu.cn

Abstract: This study aimed to quantify the bitter–astringent interactive perceived intensity (BAIPI) of green tea based on the Weber–Fechner law by two-alternative forced choice test. Caffeine, (-)-epigallocatechin-3-gallate (EGCG), and Quercetin-3-o-rutinoside (Que-rut) were identified as the key bitter–astringent compounds. Then, BAIPI values were assessed based on the concentration ratios and ranges of caffeine, EGCG, and Que-rut in green tea according to the Weber–Fechner law. The BAIPI values were further fitted to a logarithmic curve: $y_{\mathrm{BAIPIvalue}} = a \times \ln\left(x_{concentration\ of\ caffeine} - b\right) - c + IV_{\mathrm{initialBAIPIvalue}} - 1$. The constant terms a, b, and c were derived from the ratio of caffeine to EGCG, as the slope and X-intercept of the curves correlated exponentially with this ratio. The initial BAIPI value (IV) was calculated as: $IV_{\mathrm{initialBAIPIvalue}} = 18.7960 - 0.3956q_{(the\ ratio\ of\ caffeine\ to\ Que-rut)}$. Validation showed a standard error of 1.5865 between estimated and actual BAIPI values. This method enables the estimation of bitter–astringent intensity in green tea by analyzing the concentrations of caffeine, EGCG, and Que-rut.

Keywords: astringency; bitterness; green tea; interactive perceived intensity; quantification curve; Weber–Fechner law

check for updates

Received: 28 February 2025
Revised: 7 April 2025
Accepted: 8 April 2025
Published: 9 April 2025

Citation: Li, S.; Du, D.; Cheng, S.; Wei, Z. Evaluating the Intensity of Bitter–Astringent Interactive Perception in Green Tea Based on the Weber–Fechner Law. *Chemosensors* **2025**, *13*, 137. https://doi.org/10.3390/chemosensors13040137

Copyright: © 2025 by the authors. Licensee MDPI, Basel, Switzerland. This article is an open access article distributed under the terms and conditions of the Creative Commons Attribution (CC BY) license (https://creativecommons.org/licenses/by/4.0/).

1. Introduction

Tea, as the most widely consumed beverage globally following water, has unique flavor profiles [1]. Tea's distinct flavor arises from secondary metabolites—flavonoids, phenolic acids, and alkaloids—in tender leaves, which also contribute to bitterness and astringency [2,3]. Green tea, as a non-fermented tea, retains the highest concentration of these secondary metabolites due to manufacturing process, thereby preserving more significant bitterness and astringency, which are the key to affect the choice of consumers [2,4,5].

Bitterness is a basic taste produced by the activation of taste receptors encoded by the TAS2Rs gene when the bitter tastants in tea entering the oral cavity [2,6]. The compounds responsible for bitterness in green tea are mainly caffeine and catechins [2], which can enhance the umami taste of green tea caused by theanine [7] and relieve the sweetness of desserts when drinking green tea [4,8]. Astringency refers to a characteristic drying, rough, or puckery sensation in the oral cavity that arises from two distinct mechanisms: (1) the physicochemical interaction between polyphenols and salivary proteins/mucosal pellicle proteins, leading to precipitation and reduced oral lubrication [2,5,9]; or (2) a trigeminal nerve-mediated sensation triggered when astringents activate G protein-coupled receptor signaling pathways in trigeminal ganglion cells [10]. This complex sensory phenomenon involves both physical protein–tannin interactions and neural sensory transduction pathways.

Astringency enhances the sweet aftertaste (Huigan) of tea [5] and influences retronasal aroma perception [11]. Additionally, the bitter and astringent perception of consumers varied due to genetic differences in taste receptors and receptor expression [6]. Therefore, it is urgent to develop a standardized quantitative scale for the intensity of bitterness and astringency in green tea to help consumers choose products that suit their taste preferences.

Previous studies have employed two primary approaches to measure bitterness and astringency in green tea: conventional and intelligent sensory evaluation. Conventional sensory evaluation is to assess the level of bitterness and astringency through subjects rating samples using standardized taste solutions as references [8,12–14]. However, variability in reference solution concentrations across studies prevents unified intensity standards. Intelligent sensory evaluation is mainly to quantify bitter and astringent intensity through electrochemical [15], optical [16], mass [5], and biological [17] sensing techniques based on the reaction of taste compounds with the corresponding receptors or saliva in the oral cavity. However, it fails to directly link instrumental signals to human perceptual experience [18,19].

The Weber–Fechner law is central to the field of psychophysics in quantifying the internal perceptual intensity of external stimuli, specifically that the psychological perceptual intensity of a stimulus is proportional to the logarithm of the physical intensity by experimental verification [20]. At present, there were many studies to assess the internal psychological perception of taste stimuli based on the Weber–Fechner law. The sweetness index [14] and sourness index [21] of five sugars and acids were determined by converting absolute thresholds and difference thresholds obtained through triangle tests and paired comparisons based on the Weber–Fechner law. The sweetness of sucrose under different citric acid backgrounds and the sourness of citric acid under different sucrose backgrounds were calculated by fitting absolute threshold and weber fraction equations, respectively [22]. A quantitative equation for overall umami strength in foods and condiments was also defined by sensory evaluation based on the Weber–Fechner law [23]. Therefore, the perceived intensity of taste stimuli could be deduced according to the content of taste compounds. The content range and ratio of bitter and astringent compounds in green tea is defined. If the relationship between the content of bitter and astringent compounds in green tea and the perceived intensity of taste is derived based on the Weber–Fechner law, the perceived intensity of bitterness and astringency in green tea can be quantified under uniform criteria.

Additionally, the bitter and astringent perception of green tea is often inseparable for consumers [17]. Catechins have both bitterness and astringency, and caffeine and (-)-epigallocatechin-3-gallate (EGCG; the most abundant catechin in green tea) can strengthen each other's bitterness and astringency [7]. Flavonol glycosides contributed astringency to green tea and can also increase the bitterness of caffeine [24]. Moreover, a subregion within the insular cortex of the cerebral cortex exhibited responsiveness to both astringent and bitter stimuli, indicating that these inputs underwent neural information integration in the human brain to promote people to produce bitter–astringent interactive perception [25]. Therefore, the overall perceived intensity of bitterness and astringency produced by people after drinking green tea was defined as bitter–astringent interactive perceived intensity (BAIPI) in this study. To establish a universal quantification scale for BAIPI, this study is (1) to determine the concentration of bitter and astringent compounds in green tea; and then, (2) to quantify the BAIPI values of green tea and fit curves based on the Weber–Fechner law according to the concentration; and next, (3) to verify the applicability of the BAIPI quantification curve by green tea samples in the market.

2. Materials and Methods

2.1. Chemicals

The standards (alkaloids, gallic acid (GA), catechins, flavonol glycosides, and organic acids) for bitter and astringent compounds analysis, other taste indicators analysis, and sensory panel test of green tea were purchased from GlpBio Co., Ltd. (Montclair, NJ, USA). The mobile phase components for high performance liquid chromatography (HPLC) analysis consisted of formic acid (Macklin, Shanghai, China) and acetonitrile (Aladdin, Shanghai, China). Ultrapure water used in the experiments was produced by an AWL-6000-M purification system (Aquapro, FL, USA). For analysis of other taste indicators in green tea, we used a Total Carbohydrate Assay Kit (Solarbio, Beijing, China) and Amino Acid Assay Kit (Ninhydrin colorimetry method, Yuanye, Shanghai, China).

2.2. Green Tea Collection and Sample Preparation

Green tea samples were purchased from different tea factories, and the specific information is shown in Table 1. From the complete collection, we selected 11 representative green tea samples as model-samples (encompassing all fixation methods; indicated in bold italic font), while the remaining 32 samples served as the validation set. The tea leaves were crushed into particles (0.83 mm < the particle size of tea leaves $\leq$ 1 mm). Precisely 1 g of processed tea particles was combined with 100 mL of ultrapure water (maintained at 95 $\pm$ 1 °C) in a standardized 440 mL tea bowl. The mixture was homogenized using a DF-101S magnetic stirring system (Lichen Instrument, Shanghai, China) at a constant 300 rpm for exactly 3 min to produce the tea infusion.

Table 1. Data on the green tea samples used.

Name	Code	Cultivated Variety	Picking Time	Fixation Ways	Manufacturer
West Lake Long Jing Spring	WLS	Longjing 43	March 2023	Stir-frying	Hangzhou Zhijiang Tea Co. Ltd. (Zhejiang, China)
Long Jing Spring	***LJS***	***Longjing 43***	***March 2023***	***Stir-frying***	***Hangzhou LvYi Tea Industry Co. Ltd.*** (Zhejiang, China)
Long Jing Summer	***LJM***	***Longjing 43***	***June 2023***	***Stir-frying***	***Hangzhou LvYi Tea Industry Co. Ltd.*** (Zhejiang, China)
Yunwu Spring	FWS	Fuyun No.6	March 2023	Stir-frying	Fujian Runmutang Tea Manor Co. Ltd. (Fujian, China)
Yuhua before Tomb Sweeping	YBTS	Longjing 43	March 2023	Stir-frying	Nanjing Chunrun Tea Industry Co. Ltd. (Jiangsu, China)
Yuhua before Grain Rain	YBGR	Longjing 43	April 2023	Stir-frying	Nanjing Chunrun Tea Industry Co. Ltd. (Jiangsu, China)
Laoshan tea Before Grain Rain	LTB	Local population	April 2023	Stir-frying	Qingdao Lao-Tea Industry Co. Ltd. (Shandong, China)
Laoshan tea After Grain Rain	LTA	Local population	May 2023	Stir-frying	Qingdao Lao-Tea Industry Co. Ltd. (Shandong, China)
Anji White tea High grade	AWH	White Leaf No.1	March 2023	Stir-frying	Anji Bai Tea Factory (Anhui, China)
Anji White tea Low grade	AWL	White Leaf No.1	March 2023	Stir-frying	Anji Bai Tea Factory (Anhui, China)
Biluochun Spring	***BCS***	***Dongshan population***	***March 2023***	***Stir-frying***	***Shandong YIBEIXIANG Tea Industry Co. Ltd.*** (Shandong, China)
Biluochun High grade	BCH	Dongshan population	March 2023	Stir-frying	Zhejiang Yifutang Tea Industry Co. Ltd. (Zhejiang, China)
Biluochun Low grade	BCL	Dongshan population	March 2023	Stir-frying	Zhejiang Yifutang Tea Industry Co. Ltd. (Zhejiang, China)
Xinyang Maojian before Tomb Sweeping	XTS	Local population	March 2023	Stir-frying	Farmhouse Tea (Henan, China)
Xinyang Maojian before Grain Rain	XGR	Local population	April 2023	Stir-frying	Farmhouse Tea (Henan, China)

Table 1. *Cont.*

Name	Code	Cultivated Variety	Picking Time	Fixation Ways	Manufacturer
Guizhou Maojian Spring	GNS	Local Small Leaf	March 2023	Stir-frying	Guizhou Lenton Agricultural Development Co. Ltd. (Guizhou, China)
Guizhou Maofeng Spring	GMS	Fuding big white tea	March 2023	Stir-frying	Guizhou Meitan Daye Xin Tea Co. Ltd. (Guizhou, China)
Yunnan tea Spring	YTS	Yunnan Large Leaf	February 2023	Baking	Yunnan Wanhongyang Tea Co. Ltd. (Yunnan, China)
Huangshan Maofeng High grade	HMH	Huangshan Large Leaf	March 2023	Baking	Xie Yuda Tea Co. Ltd. (Anhui, China)
Huangshan Maofeng Low grade	HML	Huangshan Large Leaf	April 2023	Baking	Xie Yuda Tea Co. Ltd. (Anhui, China)
Taiping Houkui	THK	Huangshan Large Leaf	April 2023	Baking	Huangshan Mingpingxing Tea Co. Ltd. (Anhui, China)
Taiping Bujian	TBJ	Mountain Native	April 2023	Baking	Huangshan Hukeng Tea Co., Ltd. (Anhui, China)
Jingting Lvxue Tea	JLT	Southern Anhui Small Leaf	March 2023	Baking	Anhui Jingting Lvxue Tea Co. Ltd. (Anhui, China)
Liu 'an Guapian Spring	***LGS***	***Longjing 43***	***April 2023***	***Baking***	***Jinzhai County Red Xin Tea Professional Cooperative*** (Anhui, China)
Liu 'an Guapian Low grade	LGL	Dushan Small Leaf	April 2023	Baking	Anhui Lu 'an Guapian Tea Industry Co. Ltd. (Anhui, China)
Sichuan Maofeng	SMF	Huangshan Large Leaf	March 2023	Baking	Sichuan Sanhua Tea Industry Co. Ltd. (Sichuan, China)
Huangshan Maofeng Spring	***HMS***	***Huangshan Large Leaf***	***March 2023***	***Baking***	***Huangshan XIQINGFENG Agricultural Development Co. Ltd.*** (Anhui, China)
Huangshan Maofeng Summer in Last year	***HMML***	***Huangshan Large Leaf***	***June 2022***	***Baking***	***Huangshan MUFAN Trading Co. Ltd.*** (Anhui, China)
Hunan Yunwu	HYW	Small Leaf Population	April 2023	Baking	Hunan Gulou Xuefeng Yunwu Tea Co. Ltd. (Hunan, China)
Liangshan Mahu	LMH	Local population	March 2023	Sunning	Leibo county Huang Lang Tea Factory (Sichuan, China)
Sun-dried raw tea Spring	***SRS***	***Yunnan Large Leaf***	***March 2023***	***Sunning***	***Biyun Spring Tea Factory*** (Yunnan, China)
Sun-dried raw tea Spring in Last year	***SRSL***	***Yunnan Large Leaf***	***March 2022***	***Sunning***	***Yunnan Cangyuan Wa Camellia Factory Co. Ltd.*** (Yunnan, China)
Tuo Tea Spring	TTS	Yunnan Large Leaf	March 2023	Sunning	Yunnan Xiaguantuo Tea (Group) Co. Ltd. (Yunnan, China)
Dian Green Spring	DGS	Yunnan Large Leaf	March 2023	Sunning	Lancang Jing Tea Factory (Yunnan, China)
Yunnan Qingzhen Spring	YQS	Yunnan Large Leaf	March 2023	Steaming	Yunnan Wanhongyang Tea Co. Ltd. (Yunnan, China)
Enshi Gyokuro	EGK	Gyokuro	March 2023	Steaming	Enshi Huazhishan Ecological Agriculture Co. Ltd. (Hubei, China)
Enshi Gyokuro Spring	***EGS***	***Gyokuro***	***March 2023***	***Steaming***	***Enshi Chunzhihuo Tea Co. Ltd.*** (Hubei, China)
Enshi Gyokuro Spring in Last year	***EGSL***	***Gyokuro***	***April 2022***	***Steaming***	***Jinhua Jade Tea Co. Ltd.*** (Zhejiang, China)
Fried Green Tea	FGT	Uji	May 2023	Steaming	ITO Hisako Shimen Co., Ltd. (Japan)
Fukuoka Yamecha	FKY	Fukuoka	March 2023	Steaming	Kamuyuan Co., Ltd. (Japan)
Shizuoka Sencha Spring	***SSS***	***Shizuoka***	***March 2023***	***Steaming***	***Harada Tea Industry Ltd. (Japan)***
Shizuoka Kakegawa	SKK	Shizuoka	May 2023	Steaming	Ryowa Garden Co., Ltd. (Japan)
Kagoshima Chiran	KSC	Kagoshima	March 2023	Steaming	Yamashiro Co., Ltd. (Japan)

The font of model-samples is bold and italic.

2.3. Bitter and Astringent Compounds Analysis of Green Tea

The bitter and astringent compounds of green tea were determined by HPLC (Waters 1525; Milford, MA, USA) equipped with a 250 × 4.6 mm, 5 μm, Agilent 5 TC-C18 (2) column (CA, USA). All samples were filtered through 0.45 μm filters (mixed cellulose, Navigator, Tianjin, China) prior to analysis by HPLC. The determination method of alkaloids, GA, and catechins was adapted from Huang et al. [26] with modifications. A gradient elution with 0.1% formic acid as mobile phase A and acetonitrile as mobile phase B at a flow rate of

1 mL/min was performed. The gradient was carried out as follows: initial 5% B for 2 min, linear change to 13% B for 6 min, linear change to 28% B for 14 min, linear change to 95% B for 3 min, and finally linear change to 5% B for 5 min. Detection was performed at 278 nm using a Waters 2489 UV-Visible detector (Milford, MA, USA).

Flavonol glycosides were determined according to a modified method from Liu et al. [27], utilizing the following mobile phases: 0.15% formic acid in 3% acetonitrile/water (mobile phase A) and 0.15% formic acid in 30% acetonitrile/water (mobile phase B). The gradient elution (1 mL/min) was carried out as follows: 0% B, 0–20 min; 0–50% B, 20–28 min; 50–100% B, 28–47 min; 100% B, 47–55 min; 0–100% B, 55–58 min. Detection wavelength was set at 360 nm. The specific detection parameters for all target compounds are shown in Table 2.

Table 2. The detection parameters of bitter and astringent compounds.

Compounds	Perceived Types and Thresholds (mg/L)	CAS	Purity	MW	Calibration Curves α	R^2 β	Linear Range (mg/L)
Caffeine	Bitter, 97.1	58-08-02	HPLC ≥ 98	194.19	y = 23,234x + 1223.2	0.9995	13.38–462
Theobromine	Bitter, 144.1	83-67-0	HPLC ≥ 98	180.16	y = 57,560x − 11,190	0.9995	1.07–86.25
Theophylline	Bitter, not reported	58-55-9	HPLC ≥ 98	180.16	y = 48,170x − 6702.7	0.9961	0.13–13.88
Gallic acid (GA)	Astringent, 49.3	149-91-7	HPLC ≥ 98	170.12	y = 28,540x + 25,118	0.9985	1.31–31.36
(–)-Gallocatechin (GC)	Astringent, 165.39	3371-27-5	HPLC ≥ 98	306.27	y = 177.04x + 881.17	0.9996	3.25–96.84
(–)-Epigallocatechin (EGC)	Astringent, 159.26	970-74-1	HPLC ≥ 98	306.27	y = 1435x − 77,330	0.9997	115.01–684.6
(+)-Catechin (C)	Astringent, 119.01; Bitter, 249.63	154-23-4	HPLC ≥ 98	290.27	y = 6346.7x − 20,348	0.9999	10.46–311.5
(–)-Epicatechin (EC)	Astringent, 284.83; Bitter, 284.83	490-46-0	HPLC ≥ 98	306.27	y = 6247.5x − 7629.6	0.9995	31.65–188.4
(–)-Epigallocatechin-3-gallate (EGCG)	Astringent, 87.09; Bitter, 174.18	989-51-5	HPLC ≥ 98	458.37	y = 12,043x − 679,287	0.9980	131.12–780.5
(–)-Gallocatechin gallate (GCG)	Astringent, 178.76; Bitter, 178.76	4233-96-9	HPLC ≥ 98	458.37	y = 11,012x − 81,486	0.9979	10.46–62.3
(–)-Epicatechin-3-gallate (ECG)	Astringent, 115.02; Bitter, 79.63	1257-08-5	HPLC ≥ 98	442.37	y = 15,400x − 117,766	0.9993	8.24–245.25
(–)-Catechin gallate (CG)	Astringent, 110.59; Bitter, 75.20	130405-40-2	HPLC ≥ 98	442.37	y = 16,715x − 26,469	0.9978	1.59–47.6
Myricetin-3-o-rhamnoside (Myr-rha)	Astringent, 4.6	17912-87-7	HPLC ≥ 98	464.38	y = 8549.6x − 4314.5	0.9992	0.57–2.74
Quercetin-3-o-galactoside (Que-gal)	Astringent, 0.2	482-36-0	HPLC ≥ 98	464.38	y = 16,461x − 5756.4	0.9992	0.89–26.67
Quercetin-3-o-glucoside (Que-glu)	Astringent, 0.3	21637-25-2	HPLC ≥ 98	464.38	y = 18,239x − 1582.5	0.9976	0.06–10.39
Quercetin-3-o-rutinoside (Que-rut)	Astringent, 0.0007	153-18-4	HPLC ≥ 98	610.52	y = 13,286x − 5294.3	0.9995	0.91–27.25
Kaempferol-3-o-rutinoside (Kae-rut)	Astringent, 0.15	17650-84-9	HPLC ≥ 98	594.52	y = 7351.2x − 1655.8	0.9990	0.44–13.17
Kaempferol-3-o-β-D-glucoside (Kae-glu)	Astringent, 0.3	480-10-4	HPLC ≥ 98	448.38	y = 15,641x − 884.87	0.9990	0.13–3.21

α: x refers to the concentration of compounds (mg/L), and y refers to the peak area of chromatogram; β: is the goodness of fit for the calibration curves.

2.4. Matrix Composition Analysis of Green Tea

In addition to bitterness and astringency, the basic taste profile of green tea comprises sweetness, umami, and sourness. Accordingly, the matrix composition of the bitter–astringent simulation solution was designed to reflect the concentrations of sweet, umami, and sour compounds typically found in green tea. Total carbohydrate (TC) and total free amino acid (TFAA) were measured using commercial assay kits (UV-Vis spectrophotometry, WFJ 7200; Unico, Shanghai, China) at absorbance wavelengths of 540 nm and 570 nm, respectively. These metrics represent the collective sweetness (TC) and umami (TFAA) contributions in green tea. Organic acids, representing sourness, were quantified via HPLC following the method of Yu et al. [28]. Sample pretreatment and HPLC conditions aligned with Section 2.3. Detailed analytical parameters are provided in Table 3. Sucrose, theanine, and citric acid were selected as the primary matrix components for the simulation solution, as they are the most abundant sugar, amino acid, and organic acid in green tea, respectively [26,29]. Their concentrations corresponding to the levels of TC, TFAA, and total organic acids in green tea (shown in Table 4).

Table 3. The detection parameters of other taste indicators.

Taste Indicators	Calibration Curves	x	y	R^2 $^{\alpha}$	Linear Range (mg/L)
Total carbohydrate (TC)	y = 0.0006x − 0.0128	The concentration of glucose (mg/L)	The absorbance difference of spectrum	0.9973	10–500
Total free amino acid (TFAA)	y = 0.0593x + 0.0014	The concentration of amino acid standard solution (mg/L)	The absorbance difference of spectrum	0.9990	2–10
Oxalic acid	y = 13,017x − 104,627	The concentration of oxalic acid (mg/L)	The peak area of chromatogram	0.9953	14.09–208.7
Tartaric acid	y = 1383.3x − 16,178	The concentration of tartaric acid (mg/L)	The peak area of chromatogram	0.9948	10.96–121.77
Malic acid	y = 2370.2x − 4067.5	The concentration of malic acid (mg/L)	The peak area of chromatogram	0.9934	25.01–250.1
Citric acid	y = 1001x − 5925.8	The concentration of citric acid (mg/L)	The peak area of chromatogram	0.9999	46.31–385.95
Succinic acid	y = 564.49x + 9557.8	The concentration of succinic acid (mg/L)	The peak area of chromatogram	0.9946	11.52–214.25

α: The goodness of fit for the calibration curves.

Table 4. The concentration of the other taste indicators in all green tea samples.

Samples	Total Free Amino Acid (mg/L)	Total Carbohydrate (mg/L)	Oxalic Acid (mg/L)	Tartaric Acid (mg/L)	Malic Acid (mg/L)	Citric Acid (mg/L)	Succinic Acid (mg/L)	Total Organic Acids (mg/L)
LJS	36.09 ± 0.78	74.01 ± 1.61	79.71 ± 7	51.24 ± 2.26	144.85 ± 4.03	141.96 ± 8.8	109.23 ± 6.14	526.99 ± 7.52
LJM	36.32 ± 0.67	112.56 ± 3.21	91.55 ± 4.33	30.95 ± 2.52	90.89 ± 6.19	173.62 ± 7.9	112.87 ± 6.44	499.87 ± 11.4
BCS	29.13 ± 0.78	102.93 ± 1.61	81.85 ± 1.5	21.56 ± 1.01	138.65 ± 10.51	183.98 ± 6.15	111.76 ± 4.44	537.8 ± 13.05
HMS	37.22 ± 1.03	100.52 ± 2.41	99.01 ± 1.48	46.28 ± 4.81	152.32 ± 8.05	231 ± 3.7	132.53 ± 8.21	661.13 ± 9.07
HMML	23.07 ± 1.4	62.77 ± 1.61	73.64 ± 2.24	22.17 ± 1.63	33.02 ± 6.94	128.97 ± 8.89	95.85 ± 3.25	353.64 ± 5.97
LGS	23.07 ± 1.7	63.57 ± 2.41	105.6 ± 3.42	37.14 ± 2.62	76.53 ± 4.51	280.05 ± 3.6	82.33 ± 10.08	581.65 ± 12.1
SRS	29.35 ± 1.7	85.26 ± 1.61	99.84 ± 6.73	29.3 ± 2.3	63.09 ± 0.38	142.77 ± 7.87	188.67 ± 6.92	523.68 ± 16.69
SRSL	21.49 ± 0.67	49.92 ± 1.61	83.73 ± 1.24	50.4 ± 3.34	136.59 ± 2.84	123.53 ± 0.01	133.92 ± 8.01	528.17 ± 7.23
EGS	26.43 ± 1.4	55.54 ± 4.02	78.46 ± 0.75	41.7 ± 3.37	122.07 ± 1.55	131.53 ± 0.25	89.97 ± 2.79	463.74 ± 1.13
EGSL	8.74 ± 0.08	115.78 ± 3.21	158.02 ± 2.54	52.55 ± 7.53	81.14 ± 6.82	139.46 ± 3.42	92.15 ± 8.96	523.32 ± 24.08
SSS	18.57 ± 1.4	90.88 ± 2.41	111.83 ± 5.08	37.21 ± 3.75	139.26 ± 6.52	126.8 ± 1.5	78.15 ± 9.18	493.25 ± 23.55
Mean	21.77 ± 5.36	96.65 ± 10.41	86.16 ± 28.16	39.58 ± 12.85	93.02 ± 40.41	154.41 ± 66.19	103.02 ± 34.92	475.5 ± 117.73
FWS	26.14 ± 0.81	55.54 ± 0.8	113.46 ± 1.1	29.35 ± 2.05	117.39 ± 5.4	128.72 ± 9.02	72.98 ± 7.06	461.91 ± 2.96
WLS	27.56 ± 0.34	89.27 ± 0.8	107.25 ± 11.83	28.16 ± 1.16	111.59 ± 6.53	129.41 ± 8.79	110.3 ± 5.41	486.71 ± 22.34
GMS	15.93 ± 0.37	79.63 ± 2.41	73.15 ± 2.97	29.02 ± 3.75	86.86 ± 7.16	76.05 ± 7.06	76.04 ± 9.84	341.12 ± 16.92
GNS	19.81 ± 0.94	70 ± 2.41	72.54 ± 4.85	35.55 ± 1.8	144.42 ± 5.72	61.87 ± 0.63	78.36 ± 7.11	392.75 ± 6.86
XTS	15.26 ± 0.98	62.77 ± 3.21	84.31 ± 3.29	23.67 ± 1.2	116.49 ± 2.78	62.16 ± 1.42	82.69 ± 7.17	369.31 ± 8.93
XGR	18.7 ± 0.64	67.59 ± 1.61	84.04 ± 1.04	28.32 ± 6.34	118.96 ± 3.05	139.71 ± 12.42	112.05 ± 1.52	483.08 ± 4.64
YBTS	19.44 ± 0.37	78.03 ± 2.41	90.5 ± 6.36	36.04 ± 7.89	141.96 ± 9.12	202.4 ± 19.2	133.45 ± 3.06	604.36 ± 30.55
YBGR	20.38 ± 0.57	147.9 ± 4.82	71.97 ± 10.34	41.93 ± 1.7	99.38 ± 1.86	145.52 ± 7.43	72.89 ± 1.77	431.69 ± 16.71
LTB	15.6 ± 1.18	83.65 ± 1.61	81.96 ± 1.72	33.5 ± 5.22	46.58 ± 3.86	182.67 ± 7.06	17.04 ± 2.2	361.74 ± 2.41
LTA	16 ± 0.51	169.59 ± 2.41	75.14 ± 1.96	42.49 ± 1.97	41.08 ± 0.6	130.24 ± 12.03	39.71 ± 2.55	328.67 ± 12.29
AWH	37.56 ± 0.84	65.18 ± 2.41	86.54 ± 8.24	37.51 ± 5.05	147.54 ± 3.92	157.05 ± 6.37	162.08 ± 2.71	590.73 ± 8.08
AWL	23.65 ± 0.27	53.93 ± 2.41	64.47 ± 2.88	31.39 ± 4.98	116.48 ± 6.12	147.86 ± 4.21	76.65 ± 2.98	436.85 ± 13.54
BCH	25 ± 0.34	106.14 ± 3.21	34.41 ± 5.68	36.56 ± 1.48	118.05 ± 2.81	139.2 ± 7.98	77.16 ± 2.25	405.38 ± 9.48
BCL	9.47 ± 1.04	71.6 ± 0.8	75.8 ± 3.13	39.44 ± 3.12	47.48 ± 2.69	78.74 ± 2.24	158.41 ± 6.41	399.87 ± 6.32
YTS	15.23 ± 0.54	71.6 ± 2.41	53.51 ± 8.44	33.4 ± 5.13	37.64 ± 0.51	71.43 ± 2.28	109.98 ± 6.44	305.96 ± 7.68
HMH	23.21 ± 0.57	57.95 ± 1.61	54.56 ± 1.28	30.11 ± 2.06	121.91 ± 4.54	122.76 ± 2.64	114.49 ± 9.43	443.83 ± 13.36
HML	20.01 ± 0.34	70.8 ± 3.21	78.01 ± 7.06	33.21 ± 1.21	147.27 ± 8.35	89.4 ± 4.75	80.36 ± 0.81	428.25 ± 18.06
THK	36.39 ± 0.74	110.15 ± 4.02	84.61 ± 2.34	49.74 ± 4.13	115.49 ± 3.34	64.49 ± 2.78	114.33 ± 6.05	428.66 ± 14.12
TBJ	23.38 ± 0.4	159.95 ± 2.41	56.03 ± 1.76	30.33 ± 0.37	101.99 ± 4.93	86.66 ± 8.37	85.72 ± 5.03	360.72 ± 16
JLT	11.28 ± 0.51	188.06 ± 1.61	62.7 ± 3.89	31.14 ± 3.63	140.66 ± 12.23	81.41 ± 3.14	97.15 ± 3.92	413.07 ± 15.26
LGL	10 ± 0.37	155.13 ± 0.8	83.49 ± 4.7	64.21 ± 1.85	53.47 ± 4.25	170.47 ± 1.42	86.45 ± 6.96	458.1 ± 13.67
SMF	22.07 ± 0.17	120.55 ± 2.63	66.57 ± 2.33	59.36 ± 3.39	69.81 ± 4.47	220.43 ± 2.05	124.03 ± 7.47	540.21 ± 5.59
HYW	25.77 ± 0.3	147.89 ± 2.63	76 ± 6.4	63.5 ± 3.3	106.64 ± 4.61	279.3 ± 18.34	121.55 ± 8.87	646.99 ± 6
LMH	24.8 ± 0.54	143.84 ± 3.82	81.39 ± 1.68	64.16 ± 3.5	128.92 ± 4.41	273.43 ± 18.26	169.46 ± 5.59	717.37 ± 31.93
TTS	13.95 ± 0.4	133.21 ± 4.39	90.42 ± 3.31	44.26 ± 2.17	48.8 ± 6.56	224.12 ± 6.95	127.75 ± 7	535.35 ± 16.6
DGS	9.47 ± 0.24	140.8 ± 3.16	75.81 ± 4.41	27.95 ± 1.56	31.91 ± 0.17	123.42 ± 0.26	21.75 ± 0.15	280.85 ± 2.79
YQS	17.45 ± 0.47	167.14 ± 4.39	51.18 ± 0.69	24.49 ± 1.48	55.83 ± 5.72	83.4 ± 7.4	52.61 ± 5.44	267.5 ± 17.35
EGK	27.09 ± 0.74	107.89 ± 3.16	106.09 ± 6.12	51.36 ± 1.67	128.91 ± 5.75	263.86 ± 6.92	135.26 ± 5	685.48 ± 14.07
FGT	22.5 ± 0.2	107.38 ± 0.88	128.14 ± 2.24	37.7 ± 2.7	96 ± 4.82	207.76 ± 6	56.94 ± 4.09	526.54 ± 6.36
FKY	15.36 ± 0.54	107.38 ± 3.51	116.14 ± 2.68	29.84 ± 7.57	109.88 ± 10.75	71.64 ± 10.02	78.52 ± 7.27	406.03 ± 7.23
SKK	8.66 ± 0.1	113.46 ± 2.32	69.2 ± 3.32	32.21 ± 4.72	34.17 ± 1.41	155.17 ± 7.41	67.46 ± 1.79	358.2 ± 10.92
KSC	10.61 ± 0.57	83.58 ± 2.32	167.04 ± 6.07	32.74 ± 1.85	36.14 ± 3.16	207.52 ± 13.85	104.08 ± 9.28	547.52 ± 11.01
Mean	19.62 ± 7.24	91.51 ± 36.86	81.76 ± 25.2	37.9 ± 11.78	94.37 ± 38.65	143.07 ± 64.51	94.3 ± 37.01	451.4 ± 112.31

The results are reported as mean ± standard deviation of triplicate analysis.

2.5. Sensory Panel

A total of 20 experienced subjects (9 males and 11 females, from 18 to 28 years old) passed the screening and training about the test rules following an explanation of the study's purpose. Subjects were initially recruited based on surveys of health (i.e., food

allergies), interest, expressiveness, availability, attitudes toward green tea, and frequency of green tea consumption [30]. All subjects exhibited favorable attitudes toward green tea consumption and had a minimum of three years' experience in regular tea tasting, with specific expertise in green tea sensory evaluation protocols. Subsequently, screening tests to assess their sensory acuity were carried out [31]. The triangle test and ranking test of caffeine and EGCG solutions were employed to assess subjects' discrimination ability for bitter and astringent sensations, with a required accuracy rate >80%. The above test was conducted in two sessions, each lasting about two hours. Following the screening process, a two-week training program was subsequently conducted. Subjects underwent daily training consisting of three sets of 2-AFC tests with caffeine and EGCG solutions at concentration ratios of 0.5, 0.75, and 1 (targeting identification of the more astringent and bitter solution). The caffeine concentration range was 150–310 mg/L with a gradient interval of 120%, 115%, 110%, 105%, and 100%. All subjects ultimately achieved >80% correct identification rates. All subjects were instructed not to have cold symptoms, smoke, or eat for at least a half hour prior to the test.

2.6. Composition Determination of Simulation Solution

The composition of simulation solutions 1–7 is described in Section 3.1.3 in detail, and the concentration of compounds in simulation solution were consistent with those in the corresponding model-samples. A total of 7 groups of simulation solutions containing different bitter and astringent compounds were tested with 11 types of green tea based on the two-alternative forced choice (2-AFC) test. The entire testing procedure spanned 11 days, with one sample analyzed per day, and each evaluation session was completed within a 3-h time frame. The specific steps to determine the composition of simulation solution were as follows:

Step 1. The selected green tea sample was provided to the subjects in pairs with the corresponding simulation solutions 1–7 in a random order with covers at room temperature (25 ± 1 °C). Samples were divided into 20 mL in 50 mL cups marked with three random numbers.

Step 2. Subjects with a nose clip were instructed to take a small sip of the sample with their eyes closed after removing the covers, hold it in the mouth for 7–8 s and spit it out. Completing the evaluation of one sample, subjects were required to gargle with ultrapure water and have some unsalted biscuits to relieve taste bud stress for 15 min.

Step 3. The next sample was evaluated after rinsing the mouth with ultrapure water. Subjects were asked to write down the number of the sample with stronger BAIPI following the two samples tasting.

Step 4. When 11 green tea samples had been tested, it was necessary to record the number, denoted as m, at which the selection rates of the simulation solution are below 75% and above 25% [32]. The composition of the simulation solution with the largest m value was optimal. When multiple m maxima were the same, the composition of the simulation solution with the fewest compounds was optimal.

2.7. BAIPI Quantification Curves Establishment

The BAIPI quantification curves were grouped according to the compound ratios selected in Section 2.6 (Table 5). Each recombinant solution group maintained the corresponding compound concentration ratios and ranges specified in Table 6. The recombinant solution matrix contained sucrose, theanine, and citric acid at concentrations matching the average levels of total carbohydrates (TC), total free amino acids (TFAA), and total organic acids in the model samples (Table 4). Within each group, caffeine served as the

independent variable (x) for establishing the BAIPI quantification curves. And the specific steps were as follows:

Table 5. The ratio and the close ratio of caffeine, EGCG, and Que-rut in model-samples used for grouping.

Samples	The Ratio of Caffeine, EGCG, and Que-Rut	The Close Ratio of Caffeine, EGCG, and Que-Rut
SSS	9:18:1	10:20:1
EGS	45:83:1	45:85:1 45:80:1
LGS	18:33:1	20:35:1
BCS	44:78:1	45:80:1 45:75:1
HMML	44:75:1	45:75:1
EGSL	16:23:1	15:25:1 15:20:1
LJM	38:53:1	40:55:1
LJS	25:34:1	25:35:1
HMS	34:42:1	30:40:1 35:45:1 35:40:1
SRSL	12:13:1	10:10:1 15:15:1
SRS	13:13:1	10:10:1 15:15:1

Table 6. The grouping basis and limitation of the BAIPI quantification curve of green tea.

Groups	Ratio of Caffeine, EGCG, and Que-Rut	Concentration Range of Caffeine (mg/L)	Concentration Range of EGCG (mg/L)	Concentration Range of Que-Rut (mg/L)
1	10:20:1	150–240	300–480	15–24
2	10:10:1	230–240	230–240	15–24
3	15:25:1	150–310	250–517	15–21
4	15:20:1	172.5–310	230–414	11.5–21
5	15:15:1	230–310	230–310	15–21
6	20:35:1	150–310	262.5–542.5	7.5–15.5
7	25:35:1	164.25–310	230–434	6.57–12.4
8	30:40:1	172.5–310	230–413.33	5.75–10.33
9	35:45:1	178.89–310	230–398.57	5.11–8.86
10	35:40:1	201.25–310	230–354.29	5.75–8.86
11	40:55:1	167.27–310	230–426.25	4.18–7.75
12	45:85:1	153–296.47	289–560	3.4–6.82
13	45:80:1	153–310	272–551.11	3.4–6.89
14	45:75:1	153–310	255–516.67	3.4–6.89

Step 1. The lowest caffeine concentration in the selected group was used as the initial concentration, and the corresponding BAIPI value was defined as 1.

Step 2. Based on the initial concentration of caffeine, the first recombinant solution was prepared according to the proportion of compounds in this group. Subsequently, a series of recombinant solutions with varying compound concentrations within this group were established based on the lg11 increment.

Step 3. The first recombinant solution was provided to the subjects in pairs with other recombinant solutions. The tasting sequence between the two reconstituted solutions was randomized. With the first reconstituted solution held constant, the other recombinant solutions were paired with it for comparative tasting, with their presentation order following an ascending gradient of compound concentration.

Step 4. Tasting, rinsing, and recording followed Section 2.6 protocols. Until the selection rates, the first recombinant solution was less than or equal to 25% comparing with the nth recombinant solution, and the caffeine content in the nth recombinant solution was recorded as C_n.

Step 5. The BAIPI value was increased by one unit, and the caffeine concentration, denoted as C, corresponding to the updated BAIPI value was calculated according to this formula:

$$C = \sqrt{C_n \times C_{n-1}} \quad (1)$$

where C_{n-1} was the concentration of caffeine in the $n-1$th recombinant solution.

Step 6. The caffeine concentration C calculated in Step 5 was used as the initial concentration of the next round. Sequentially, subjects were instructed to advance to Steps 2 to 6 if all compounds were within the concentration range or to Step 7 otherwise.

Step 7. The initial caffeine concentration and the caffeine concentration C calculated in each round were recorded as the x variable, and the BAIPI value was recorded as the y variable. Subsequently, the curve was fitted for this group.

After establishing the BAIPI quantification curve for a given group, Steps 1 to 7 were repeated for the next group. In the initial group, participants performed duplicate tests—both with and without nose clips. Results indicated that nasal occlusion had no significant effect on BAIPI curve establishment ($p > 0.05$). Consequently, we omitted nose clip usage in following trials.

2.8. Initial BAIPI Values Calibration

The group of BAIPI quantification curves corresponding to the initial compound with the lowest dose-over-threshold (DoT) values was designated as 'Group r'. The DoT value represents the ratio of a compound's concentration to its corresponding perception threshold [24]. The compound concentrations associated with BAIPI values within this group was used as references to calibrate the initial BAIPI values of other groups by 2-AFC tests. The specific steps were as follows:

Step 1. A series of recombinant solutions was prepared at the compound concentrations corresponding to the BAIPI values of 'Group r'.

Step 2. The recombinant solution described in Step 1 was provided to the subjects one by one in ascending order of BAIPI values. Concurrently, the first recombinant solution from each group (as described in Section 2.7) was also provided to subjects as a comparison sample. These solutions were presented in ascending order according to their initial compound DoT values.

Step 3. Tasting, rinsing, and recording followed Section 2.6 protocols. The BAIPI value of the recombinant solution in 'Group r' with the selection rates exceeding 25% but below 75% was the initial BAIPI value of the other group in the pairing comparison.

Step 4. When the selection rate remained at 25% or lower following the tests of all recombinant solutions in 'Group r', the group with the highest initial BAIPI value was chosen as a new 'Group r'. Steps 1 to 4 were repeated until the initial BAIPI values standardization was completed across all groups.

2.9. Direct Assessment for BAIPI Values

The concentration of bitter and astringent compounds corresponding to BAPI values at certain intervals was used as the scale (the specific scale was described in Section 3.4). Subjects underwent a three-week training period to become acquainted with the varying levels of bitter and astringent intensity. Subsequently, a 9-point intensity scale (1 = lowest, 9 = highest) was used for direct evaluation. The specific steps of providing samples, tasting, and gargling were carried out according to Section 2.6.

3. Results

3.1. Bitter–Astringent Simulation Solution of Green Tea

3.1.1. Bitter Compounds Analysis of Green Tea

Figure 1 shows the concentration of bitter and astringent compounds in green tea, as detected by HPLC, along with their corresponding bitter (red dashed line) and astringent (blue dotted line) perceived thresholds. Bitterness in green tea is mainly caused by alkaloids and catechins [2]. The primary alkaloids in green tea are caffeine, theobromine, and theophylline. Caffeine accounts for over 90% of the total alkaloid content and was the only alkaloid exceeding the bitter threshold (Figure 1A). In Figure 1B,C, the levels of theobromine and theophylline in green tea samples were very low. Theophylline's threshold was not found, but quantitative structure-activity relationship analysis suggests its content was below the threshold [33,34].

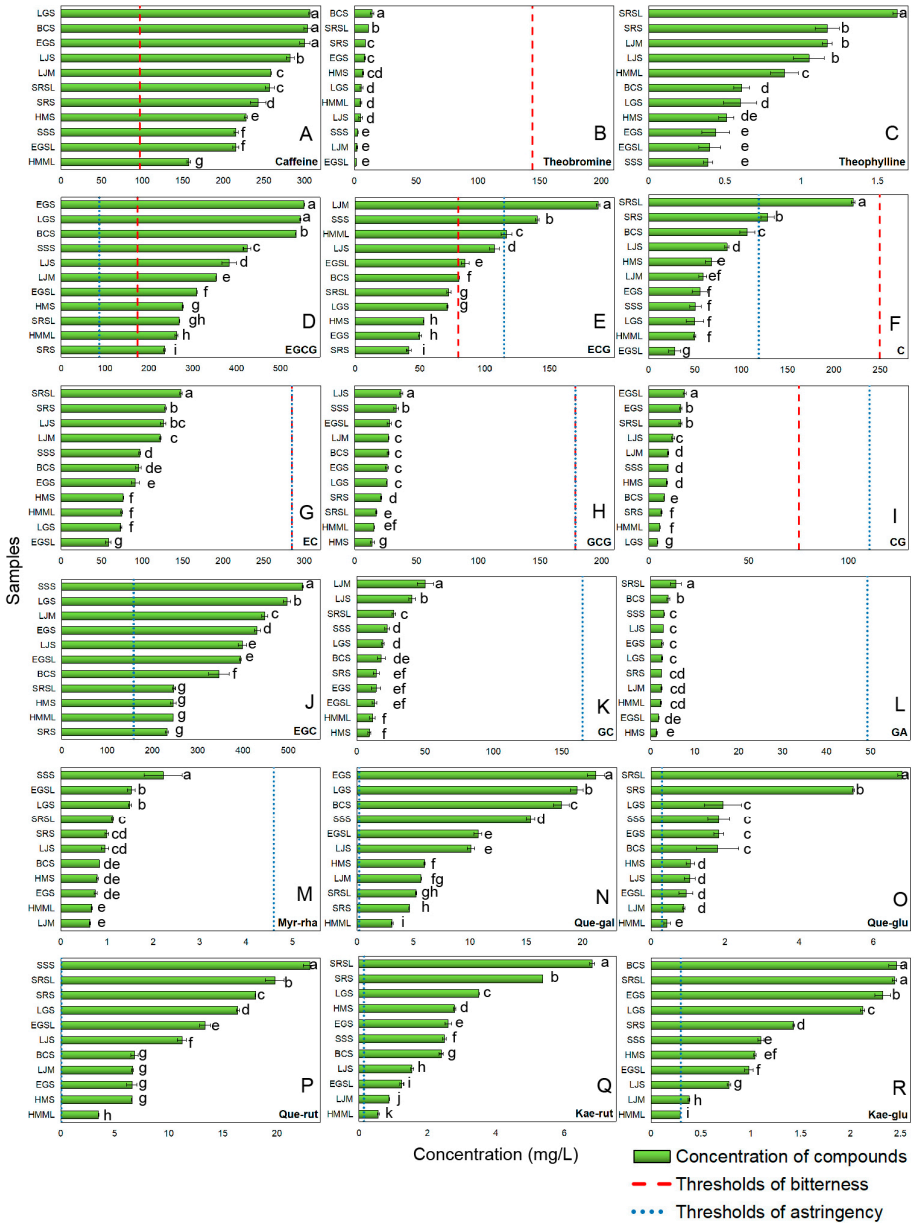


Figure 1. The concentration and perceived thresholds of bitter and astringent compounds (**A**) Caffeine; (**B**) Theobromine; (**C**) Theophylline; (**D**) EGCG; (**E**) ECG; (**F**) C; (**G**) EC; (**H**) GCG; (**I**) CG; (**J**) EGC; (**K**) GC; (**L**) GA; (**M**) Myr-rha; (**N**) Que-gal; (**O**) Que-glu; (**P**) Que-rut; (**Q**) Kae-rut; (**R**) Kae-glu in model samples. (Error lines were based on standard deviation; 'a–k' referred to the significant differences

between the groups were determined by one-way ANOVA analysis based on Duncan's multiple range test at $p \leq 0.05$).

Most of catechins contribute to both bitterness and astringency [2], including EGCG, (–)-epicatechin-3-gallate (ECG), (+)-catechin (C), (–)-epicatechin (EC), (–)-gallocatechin gallate (GCG), and (–)-catechin gallate (CG) (Figure 1). EGCG (65% of total catechins [35]) exceeded bitter and astringent thresholds in all samples (Figure 1D). ECG surpassed the bitter threshold in half of the samples but only exceeded the astringency threshold in three (Figure 1E), likely due to fewer hydroxyl groups on its B-ring compared to EGCG [2,36]. Non-galloylated catechins (C and EC) have higher thresholds than galloylated ones [2,36]. Only two green tea samples exceeded the astringency threshold (119.01 mg/L) for C (Figure 1F). EC showed a similar distribution to C, suggesting minimal impact on the bitterness and astringency (Figure 1G). GCG and CG were present in low amounts (Figure 1H,I) due to their conversion to EGCG and ECG at high temperatures [37,38].

3.1.2. Astringent Compounds Analysis of Green Tea

Catechins, phenolic acids, and flavonol glycosides mainly contribute to the astringency of green tea [2,29]. Apart from the above catechins, (-)-Epigallocatechin (EGC) and (-)-gallocatechin (GC) can only provide astringency to green tea, likely because they weakly interact with bitter receptors [36]. EGC (second most abundant after EGCG) exceeded its astringent threshold (159.26 mg/L) (Figure 1J). GC (a minor catechin) fell below the threshold due to processing losses [38] (Figure 1K). GA (linked to astringency, sourness, and sweet aftertaste [2]) had concentrations < 10 mg/L, making its contribution negligible (Figure 1L). Flavonol glycosides with extremely low astringent thresholds can impart a silky astringency to green tea [2]. All flavonol glycosides except for myricetin-3-o-rhamnoside (Myr-rha) (Figure 1M) exceeded thresholds (Figure 1N–R). In summary, 9 compounds contributed significantly to the bitterness and astringency of green tea, which were caffeine, EGCG, ECG, EGC, Quercetin-3-o-galactoside (Que-gal), Quercetin-3-o-glucoside (Que-glu), Quercetin-3-o-rutinoside (Que-rut), Kaempferol-3-o-rutinoside (Kae-rut), and Kaempferol-3-o-β-D-glucoside (Kae-glu).

3.1.3. Composition of Bitter–Astringent Simulation Solution

Additionally, the contribution of the 9 compounds to the overall bitter and astringent profiles of green tea was determined by 2-AFC test. Simulation solution 1 contained all 9 compounds. Simulation solutions 2 to 7 were created by progressively removing the compound with the lowest DoT value from the previous solution, while maintaining at least one representative from each perceived type. Finally, simulation solution 7 was composed of caffeine, EGCG, and Que-rut. According to the 2-AFC test results between green tea samples and simulation solutions in Table 7, the selection rates of simulation solutions 1, 2, and 3 were nearly all greater than or equal to 75%. This indicates that nearly all subjects perceived the simulation solution as exhibiting significantly greater bitterness and astringency ($\alpha \leq 0.05$) [32]. This may be attributed to GA, non-galloylated catechins, and galloylated catechin hydrolysis products in green tea, which likely reduce BAIPI through sweet aftertaste effects [2,29]. Five green tea samples showed no significant difference ($\alpha > 0.05$) in bitter and astringent intensity compared to simulation solution 4 and 5, with selectivity ranging from 25% to 75%. Simulation solutions 6–7 matched over 80% of samples after removing Kae-rut and Que-gal and 9 out of the 11 green tea samples showed no significant difference in bitter and astringent intensity from simulated solutions 6 and 7. Therefore, the minimal 3-compound combination (caffeine, EGCG, Que-rut) in solution 7 was identified as optimal. This result was similar to the taste reconstitution and omission experiment of black tea in the study of [24] and our study extends prior work by specifically

examining individual flavonol glycosides' effect. Meanwhile, caffeine, EGCG, and Que-rut were used to develop recombinant solutions for BAIPI quantification curves.

Table 7. The percentage of responses considering the simulation solution more bitter and astringent compared to samples (n = 20).

Samples	Simulation Solution 1	Simulation Solution 2	Simulation Solution 3	Simulation Solution 4	Simulation Solution 5	Simulation Solution 6	Simulation Solution 7
LJS	85	80	75	35	15	55	35
LJM	80	75	85	25	20	50	45
BCS	80	70	75	20	20	35	25
HMS	75	80	65	40	35	65	40
HMML	90	75	85	75	60	75	65
LGS	85	70	65	25	25	70	50
SRS	95	80	75	35	65	70	55
SRSL	75	80	70	70	55	75	45
EGS	85	75	80	20	10	65	25
EGSL	80	90	85	25	35	60	55
SSS	75	65	75	45	25	55	60

Numbers highlighted in red (25 < x < 75) in the table denote no statistically significant difference between the two samples ($\alpha > 0.05$).

3.2. BAIPI Quantification Curves in Green Tea

According the actual ratio of caffeine, EGCG, and Que-rut in model-samples (Table 5), 14 groups with similar ratios were selected to construct BAIPI quantification curves (Table 6). Table 8 shows the BAIPI quantification curves for different groups divided based on the ratio of caffeine, EGCG, and Que-rut of model-samples. When the BAIPI value of Group 2 reached 2, the concentration of caffeine, EGCG, and Que-rut exceeded the content range of model-samples specified in Table 6. As a result, it was not feasible to establish the curve in Group 2. Logarithmic curve fitting for several BAIPI plots across different groups showed that they all followed the same equation form, except for Group 2:

$$y = a \times \ln(x - b) - c \quad (2)$$

where a, b, and c were constants, x was the concentration of caffeine in this group, and y was the value of BAIPI. It can be observed that all parameter values of a are greater than zero ($a > 0$), indicating a positive correlation between BAIPI values and caffeine concentration, where larger magnitudes of a correspond to accelerated rates of BAIPI change. The parameter b defines the effective concentration threshold of caffeine, as the logarithmic term $\ln(x - b)$ requires $x > b$ to maintain mathematical validity. The parameter c modulates the vertical offset of the baseline, effectively shifting the entire dose-response curve to calibrate BAIPI reference values. As caffeine concentration approaches b ($x \to b^+$), BAIPI values plummet, reflecting heightened sensitivity to minimal concentration variations. When caffeine concentration substantially exceeds b ($x \gg b$), the growth rate of BAIPI diminishes progressively due to the asymptotic nature of logarithmic functions, ultimately approaching saturation.

The goodness of fit (R^2) and adjusted R^2 of the other groups were greater than 0.99, and the standard error of estimate (SEE) and residual sum of squares (RSS) were less than 0.3, indicating that a high level of curve fitting and predictive accuracy. However, in this study, the Weber fraction increased with BAIPI values (Figure 2A–D), indicating reduced perceptual sensitivity at higher BAIPI levels. This phenomenon also appeared in the study to determine the human sweetness and sourness interactive response [22]. This could be attributed to the interactive effect of the two sensations, resulting in alterations to the

Weber fraction when the intensity of stimulation surpassed a certain threshold [7,22,24,39]. Equation (2) conformed to the complete form of Fechner law [39], which indicated that the interactive perceived intensity of the two sensations (e.g., bitterness and astringency) conformed to the Weber–Fechner law.

Table 8. The specific information of BAIPI quantification curves of green tea.

Group	Code of Curve	m^{α}	n^{β}	Equation	$R^{2\,\gamma}$	Adjust R^2	SEE $^{\delta}$	RSS $^{\varepsilon}$
Group 1	Fit curve 1	10:20:1	0.50	$y = 3.21 \times \ln(x - 142.4) - 5.47$	0.9969	0.9960	0.1920	0.2580
Group 2	Fit curve 2	10:10:1	1.00	-	-	-	-	-
Group 3	Fit curve 3	15:25:1	0.60	$y = 4.20 \times \ln(x - 120.17) - 13.3$	0.9993	0.9991	0.0833	0.0416
Group 4	Fit curve 4	15:20:1	0.75	$y = 2.90 \times \ln(x - 155.98) - 6.95$	0.9970	0.9958	0.1592	0.1268
Group 5	Fit curve 5	15:15:1	1.00	$y = 4.20 \times \ln(x - 183.86) - 15.13$	0.9981	0.9968	0.1062	0.0338
Group 6	Fit curve 6	20:35:1	0.57	$y = 3.56 \times \ln(x - 121.79) - 10.87$	0.9991	0.9988	0.0852	0.0363
Group 7	Fit curve 7	25:35:1	0.71	$y = 3.69 \times \ln(x - 137.43) - 11.22$	0.9988	0.9983	0.0999	0.0499
Group 8	Fit curve 8	30:40:1	0.75	$y = 4.24 \times \ln(x - 137.59) - 14.11$	0.9990	0.9986	0.0905	0.0410
Group 9	Fit curve 9	35:45:1	0.78	$y = 2.90 \times \ln(x - 161.77) - 7.05$	0.9970	0.9958	0.1593	0.1268
Group 10	Fit curve 10	35:40:1	0.88	$y = 4.42 \times \ln(x - 157.55) - 15.74$	0.9987	0.9980	0.0960	0.0369
Group 11	Fit curve 11	40:55:1	0.73	$y = 3.64 \times \ln(x - 140.55) - 11.04$	0.9988	0.9983	0.1019	0.0519
Group 12	Fit curve 12	45:85:1	0.53	$y = 3.79 \times \ln(x - 126.73) - 11.44$	0.9991	0.9988	0.0960	0.0552
Group 13	Fit curve 13	45:80:1	0.56	$y = 3.56 \times \ln(x - 124.22) - 10.94$	0.9991	0.9988	0.0852	0.0363
Group 14	Fit curve 14	45:75:1	0.60	$y = 4.64 \times \ln(x - 111.1) - 16.28$	0.9991	0.9988	0.0940	0.0530

α—the concentration ratio of caffeine, EGCG, and Que-rut; β—the concentration ratio of caffeine and EGCG; γ—goodness of fit; δ—standard error of estimate; ε—residual sum of squares.

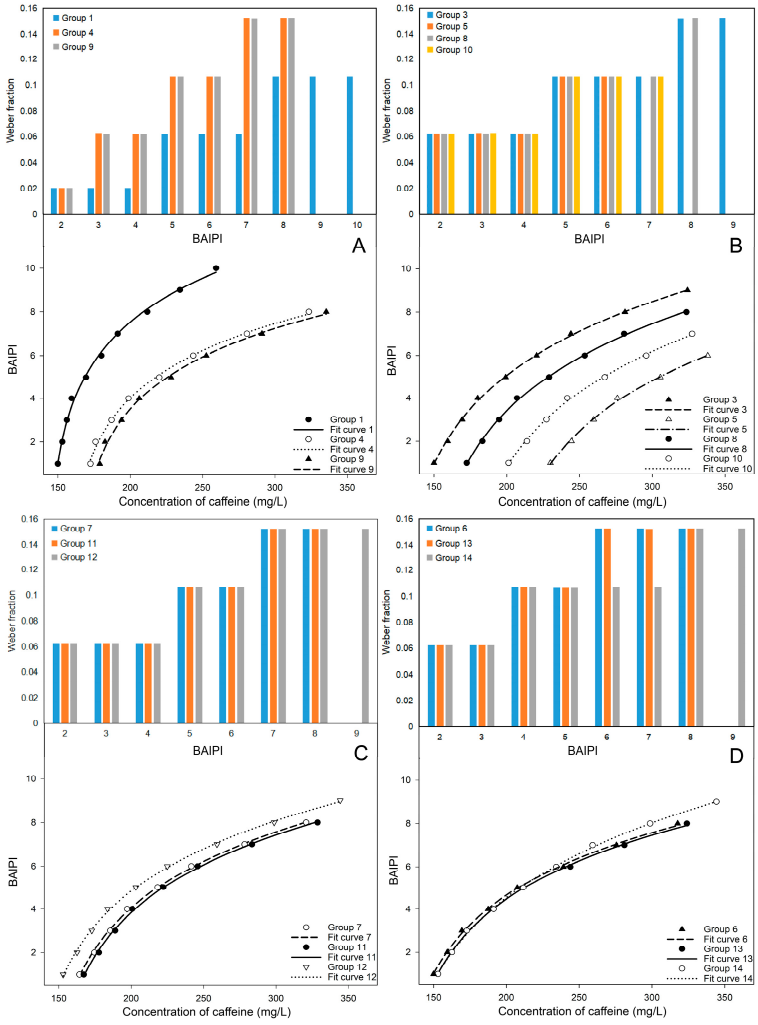


Figure 2. The Weber fraction and fit curves for 13 groups of BAIPI quantification curves (**A**) Group 1, 4 and 9; (**B**) Group 3, 5, 8 and 10; (**C**) Group 7, 11 and 12; (**D**) Group 6, 13 and 14.

3.2.1. X-Intercept of Curves

In Figure 2A, Groups 1, 4, and 9 showed an initial Weber fraction of 0.02. Groups 4 and 9 exhibited identical trends in Weber fraction changes. Additionally, it was also observed that fit curves 4 and 9 had similar degree of curvature and inclination, while fit curve 1 was quite different from them. In Figure 2B, a similar phenomenon was also observed in Groups 3, 5, 8, and 10, where the change of Weber fraction and the curvature and inclination of fit curves were similar. However, a distinct observation was the gradual rightward shift along the X-axis of fit curves 3, 8, 10, and 5 as the ratio of caffeine and EGCG (n) increased. In Figure 2C, fit curves 12, 7, and 11 were also arranged in sequence along the X-axis, with the corresponding n being 0.53, 0.71, and 0.73, respectively. Among them, the position of fit curves 7 and 11 in the figure was closer due to the n of Groups 7 and 11 was relatively close. The n of Groups 13, 6, and 14 were very close, about 0.58, resulting in their nearly overlapping positions in Figure 2D. Therefore, the curvature and inclination of the fit curve was correlated with the change trend of Weber fraction, and the position of the fit curve on the X-axis was closely associated with n.

Figure 3A shows the BAIPI value points and fit curves of all groups, and it was found that the fit curve gradually shifted to the right with the increase of n in general. This phenomenon appeared due to the gradual increase of n from 0.5 to 1.0, where the molecular quantities of caffeine and EGCG approached stoichiometric equilibrium. Under these conditions, caffeine and EGCG preferentially formed 2:2 heterotypic complexes [40]. These complexes competitively inhibited EGCG's binding affinity for salivary proteins, thereby attenuating astringency perception [41]. To maintain equivalent BAIPI values, compensatory elevation of total caffeine concentration (x) became requisite to achieve parity in overall sensory stimulation. The X-intercept, as an approximate indicator of the position of the fit curve on the X-axis, was used to conduct a correlation analysis with the n of all groups as shown in Figure 3B. It was found that the correlation fitted into exponential curves, and the equation form was as follows:

$$IC = 123.0742 + 3.3603 \times \exp 3.3852n \quad (3)$$

where n was the ratio of caffeine and EGCG in different groups, and IC was the X-intercept of the fit curve. The IC value, representing the caffeine concentration required to achieve a null BAIPI (relatively complete bitter–astringent suppression), exhibited an exponential amplification relationship with n. Specifically, at n = 0.5, $IC \approx 141.2$ mg/L; at n = 1.0, $IC \approx 222.5$ mg/L. This 57% increase in IC despite caffeine proportion doubling revealed a nonlinear caffeine-mediated bitter–astringent suppression efficacy reduction. The R^2 and SEE of the exponential curve were 0.9786 and 3.6627, respectively, indicating a strong correlation between n and X-intercept of the fit curve. The X-intercept of Equation (2) was as follows:

$$IC = \exp(c/a) + b \quad (4)$$

Substitute Equation (3) into Equation (4), the constant term c of Equation (2) could be calculated according to the following equation:

$$\exp(c/a) + b = 123.0742 + 3.3603 \times \exp 3.3852n \quad (5)$$

$$c = a \times \ln(123.0742 + 3.3603 \times \exp 3.3852n - b) \quad (6)$$

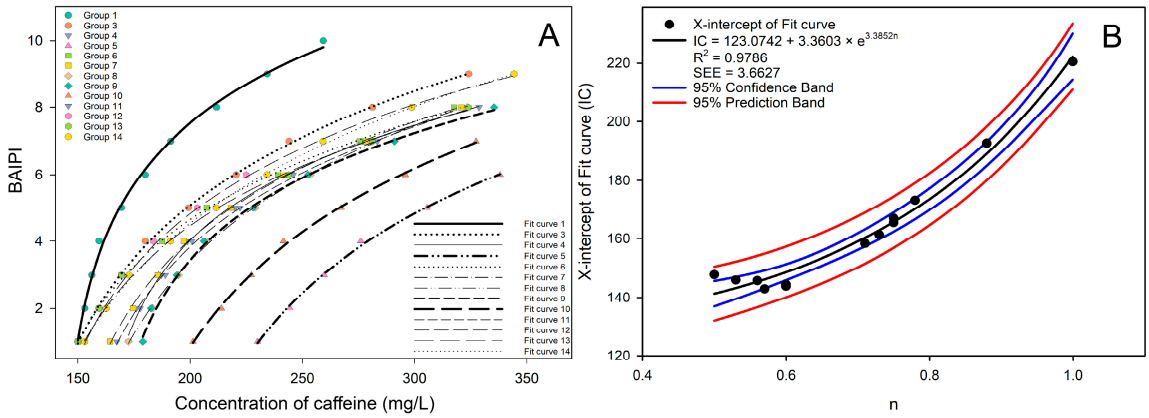


Figure 3. All the fit curves (**A**) and the correlation analysis between the concentration ratio of caffeine and EGCG and the X-intercept (**B**) for 13 groups of BAIPI quantification curves.

3.2.2. Slope of Curves

It was difficult to observe the regularity for the curvature and inclination of fit curves in Figure 3A, so an attempt was made to establish a correlation between the n and the slopes at different points of all the fit curves. Since the b of fit curve 5 was 183.86 (requiring N of ln N to be greater than 0), the slopes of the fitted curves at x = 190, 200, and 210 were calculated for correlation analysis with the n, which conformed the exponentially correlation (Figure 4A–C):

$$k_{190} = 0.0639 + 3.8717 \times 10^{-8} \times \exp 16.5879n \quad (7)$$

$$k_{200} = 0.0495 + 5.5375 \times 10^{-6} \times \exp 10.544n \quad (8)$$

$$k_{210} = 0.0420 + 2.0690 \times 10^{-5} \times \exp 8.6555n \quad (9)$$

where k was the slope of the fit curve at x = 190, 200, and 210. As x increased (from 190 to 210), the exponential coefficient decreased (from 16.5879 to 8.6555), indicating that in the high-concentration range, the sensitivity of k to n is reduced.

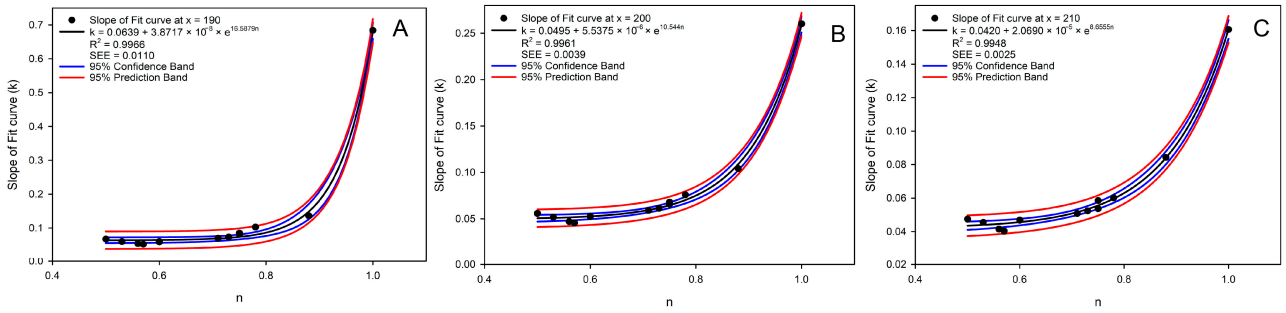


Figure 4. The correlation analysis between the concentration ratio of caffeine and EGCG and the slope at x = 190 (**A**), 200 (**B**), and 210 (**C**) for 13 groups of BAIPI quantification curves.

The R^2 of the above exponential curves were 0.9966, 0.9961, and 0.9948, respectively, and the SEEs were 0.0110, 0.0039, and 0.0025, respectively. The R^2 for the slope of the fit curve at the point following x = 220 was lower than 0.99, so the slopes of the three points were used to calculate a and b of Equation (2). Additionally, the slope of the fit curve at x = x_0 was as follows:

$$k_{x_0} = a/(x_0 - b) \quad (10)$$

Substitute Equations (7)–(9) into Equation (10), the constant term a and b of Equation (2) could be calculated according to the following equation:

$$a/(190-b) = 0.0639 + 3.8717 \times 10^{-8} \times \exp 16.5879n \quad (11)$$

$$a/(200-b) = 0.0495 + 5.5375 \times 10^{-6} \times \exp 10.544n \quad (12)$$

$$a/(210-b) = 0.0420 + 2.0690 \times 10^{-5} \times \exp 8.6555n \quad (13)$$

Equations (10)–(12) were combined in pairs, and the n values of all groups were substituted into to calculate a and b. These values then substituted into Equation (6) to calculate the corresponding c, as shown in Table 9. It was found that only the a and b values calculated by the combination of Equations (12) and (13) could substituted into Equation (6), so a and b were:

$$a = \frac{20790 + 2.3258 \times \exp 10.544n + 10.2416 \times \exp 8.6555n + 0.0011 \times \exp 19.1995n}{7500 + 5.5375 \times \exp 10.544n - 20.69 \times \exp 8.6555n} \quad (14)$$

$$b = \frac{1080000 - 4344.9 \times \exp 8.6555n + 1107.5 \times \exp 10.544n}{7500 + 5.5375 \times \exp 10.544n - 20.69 \times \exp 8.655n} \quad (15)$$

Table 9. Different sets of equations solving a, b and c of Equation (2).

n^{α}	Equations (6), (11) and (12)			Equations (6), (11) and (13)			Equations (6), (12) and (13)		
	a	***b***	***c***	***a***	***b***	***c***	***a***	***b***	***c***
0.50	2.40	152.47	-	2.72	147.47	-	3.14	137.86	3.91
0.53	2.48	151.30	-	2.81	146.23	-	3.23	136.62	6.13
0.56	2.59	149.70	-	2.92	144.65	−0.66	3.34	135.27	7.74
0.57	2.64	149.05	-	2.96	144.03	2.32	3.37	134.81	8.21
0.60	2.81	146.59	2.08	3.12	141.84	6.00	3.50	133.45	9.53
0.71	4.28	127.95	14.87	4.12	130.25	14.01	3.97	133.11	13.09
0.73	4.74	123.19	17.44	4.35	128.71	15.35	4.01	134.91	13.35
0.75	5.21	119.35	19.97	4.54	128.33	16.45	4.02	137.54	13.42
0.78	5.70	118.77	22.45	4.70	131.23	17.22	3.99	142.96	13.18
0.88	4.07	162.61	13.34	3.87	163.93	12.50	3.65	166.04	11.48
1.00	4.19	183.87	15.28	4.21	183.84	15.35	4.12	183.73	15.06

α: The concentration ratio of caffeine and EGCG.

3.3. Initial BAIPI Values Calibration of Quantification Curves

The initial BAIPI values of all quantification curves were calibrated using 2-AFC tests (Table 10). While previous studies on taste intensity quantification typically used absolute thresholds as starting points [14,42,43], this approach may not adequately represent the actual concentration ranges of compounds in specific foods, potentially introducing bias in practical applications [44]. Therefore, the minimum concentration of compounds found in green tea was employed as the quantification baseline in this research. Based on the perceived thresholds and concentration of caffeine, EGCG, and Que-rut in Tables 2 and 6, Group 14 (with the lowest initial compound DoT values) was designated as the first reference group ('Group r'). Groups 6–13 were calibrated against 'Group r' via 2-AFC tests (Table 10). Groups 6 and 7 showed the highest initial BAIPI value (9), qualifying them as potential new reference groups and Group 6 was selected to be the new 'Group r' because its DoT values were closer to the remaining groups. Thus, the initial BAIPI values of Groups 1–5 were then calibrated against the new 'Group r'. A linear correlation was

observed between the initial BAIPI values of all groups and the ratio of caffeine to Que-rut (q) (Figure 5):

$$IV = 18.7960 - 0.3956q \quad (16)$$

where q was the ratio of caffeine and Que-rut of different groups, and IV was initial BAIPI values.

Table 10. Standardized BAPI values.

q^{α}	Group	BAPI Values																							
45	1	14	1	2	3	4	5	6	7	8	9														
45	1	13	1	2	3	4	5	6	7	8															
45	1	12	1	2	3	4	5	6	7	8	9														
40	1	11			3	4	5	6	7	8	9	10													
35	1	10						6	7	8	9	10	11	12											
35	1	9					5	6	7	8	9	10	11	12											
30	1	8						6	7	8	9	10	11	12	13										
25	1	7									9	10	11	12	13	14	15	16							
20	1	6									9	10	11	12	13	14	15	16							
15	1	5															15	16	17	18	19	20			
15	1	4													13	14	15	16	17	18	19	20			
15	1	3												12	13	14	15	16	17	18	19	20			
10	1	1															15	16	17	18	19	20	21	22	23	24

α: The concentration ratio of caffeine and Que-rut.

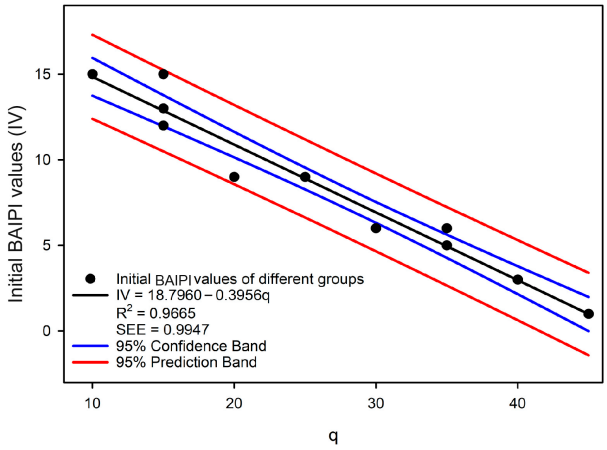


Figure 5. The correlation analysis between the concentration ratio of caffeine and Que-rut and the initial BAIPI values for 13 groups of BAIPI quantification curves.

The R^2 of the linear correlation model was 0.9665, and the SEE was 0.9947, indicating that the model was acceptable. Since the initial BAIPI value of all the fit curves in Table 8 was set to 1, the Equation (2) should be modified as follow:

$$y = a \times \ln(x - b) - c + IV - 1 \quad (17)$$

3.4. Verification of BAIPI Quantification Curves in Green Tea

The applicability of the BAIPI quantification curve was assessed through correlation analysis between calculated and directly assessed BAIPI values (Figure 6). The concentration of caffeine, EGCG, and Que-rut of green tea samples were input into Equations (6) and (14)–(16) calculated the corresponding a, b, c and IV. These parameters were then substituted into Equation (17) to calculate final BAIPI values (Table 11). Direct assessment of BAIPI values was based on a 9-point intensity scale (1 = lowest, 9 = highest). Scale reference points corresponded

to the concentration of caffeine, EGCG, and Que-rut corresponding to the BAIPI values of 1, 3, 6 (in Group 14), 9, 12, 15 (in Group 6), 18, 21 and 24 (in Group 1) in Table 10. In Figure 6, the R^2 of the correlation model based on the model, validation and all samples were 0.9475, 0.9418 and 0.9439, respectively, and SEEs were 1.4537, 1.5865 and 1.5099, respectively. These results demonstrate the model's ability to reliably estimate the comprehensive bitter–astringent perception in green tea.

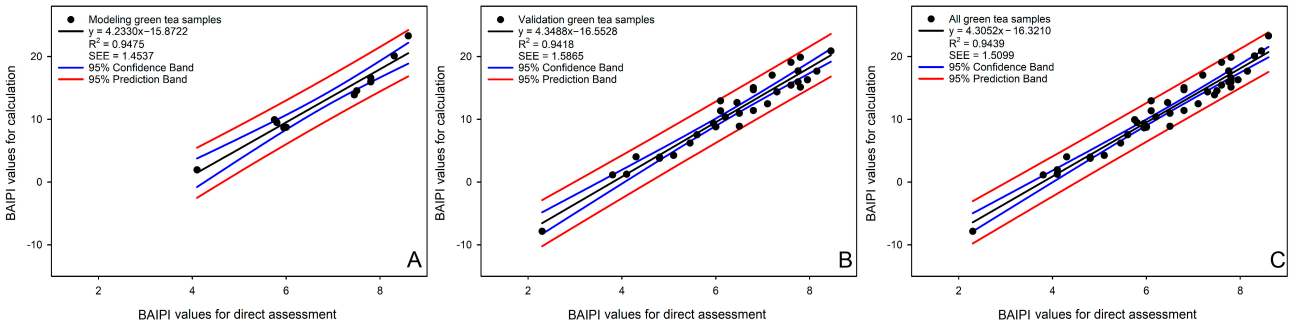


Figure 6. The correlation analysis between the BAIPI values calculated by BAIPI quantification curves and those obtained by direct assessment based on model (**A**), validation (**B**), and all samples (**C**).

Table 11. BAIPI values calculated by BAIPI quantification curves and those obtained by direct assessment.

Samples	Concentration of Caffeine (x, mg/L)	m^{α}	n^{β}	q^{γ}	$y = a \times \ln(x - b) - c + IV - 1$				BAIPI Values for Calculation (y)	BAIPI Values for Direct Assessment
					IV	*a*	*b*	*c*		
Model										
LJS	282.31	25:34:1	0.74	25	8.91	4.02	136.12	13.41	14.54	7.5
LJM	258.74	38:53:1	0.73	38	3.76	4.01	134.91	13.35	8.73	6
BCS	303.93	44:78:1	0.57	44	1.39	3.37	134.81	8.21	9.49	5.8
HMS	227.70	34:42:1	0.82	34	5.35	3.86	152.08	12.41	8.63	5.95
HMML	157.18	44:75:1	0.60	44	1.39	3.50	133.45	9.53	1.94	4.1
LGS	306.55	18:33:1	0.56	18	11.68	3.34	135.27	7.74	20.09	8.3
SRS	235.81	13:13:1	1.00	13	13.65	4.12	183.73	15.06	13.89	7.45
SRSL	257.26	12:13:1	0.96	12	14.05	3.78	179.44	12.88	16.61	7.8
EGS	300.35	45:83:1	0.54	45	0.99	3.26	136.18	6.70	9.94	5.75
EGSL	215.27	16:23:1	0.70	16	12.47	3.94	132.50	12.90	15.95	7.8
SSS	215.57	9:18:1	0.51	9	15.24	3.17	137.46	4.77	23.28	8.6
Validation										
FWS	283.56	20:22:1	0.91	20	10.88	3.63	171.33	11.54	15.44	7.6
WJS	306.13	26:37:1	0.70	26	9.30	3.92	132.32	12.82	15.05	6.8
GMS	213.78	33:56:1	0.60	33	5.74	3.50	133.47	9.52	10.37	6.2
GNS	192.33	34:58:1	0.59	34	5.74	3.45	134.00	9.01	9.34	5.95
XTS	269.28	60:96:1	0.62	60	−4.94	3.61	132.51	10.49	1.25	4.1
XGR	272.68	40:76:1	0.53	40	3.37	3.25	136.42	6.40	11.35	6.1
YTS	283.85	23:26:1	0.90	23	10.09	3.63	170.29	11.49	14.37	7.3
YGR	195.97	17:26:1	0.65	17	12.47	3.75	131.75	11.63	15.13	7.8
LTB	209.87	17:27:1	0.63	17	12.47	3.63	132.37	10.65	16.30	7.95
LTA	201.61	17:31:1	0.55	17	12.47	3.29	135.82	7.13	17.70	7.75
AWH	255.99	40:47:1	0.84	40	3.37	3.79	156.17	12.06	7.54	5.6
AWL	204.33	51:70:1	0.73	51	−1.38	4.01	134.99	13.36	1.13	3.8
BCH	239.47	50:72:1	0.69	50	−0.59	3.90	132.08	12.67	3.77	4.8
BCL	249.82	55:97:1	0.56	55	−2.57	3.34	135.24	7.77	4.25	5.1
YTS	306.85	55:87:1	0.64	55	−2.57	3.66	132.15	10.93	3.96	4.8
HMH	224.07	39:48:1	0.83	39	3.37	3.84	153.43	12.29	6.22	5.45
HML	232.93	35:45:1	0.76	35	6.53	4.01	139.95	13.35	8.89	6.5
THK	204.17	22:31:1	0.70	22	9.70	3.94	132.62	12.95	12.95	6.1
TBJ	277.26	15:16:1	0.92	15	13.26	3.64	174.17	11.77	17.03	7.2
JLT	228.59	26:37:1	0.71	26	8.51	3.97	133.23	13.12	12.47	7.1
LGL	206.88	22:36:1	0.60	22	10.49	3.52	133.28	9.70	14.71	6.8
SMF	216.72	45:57:1	0.78	45	0.99	3.98	143.44	13.14	4.01	4.3
HYW	250.67	37:47:1	0.78	37	4.55	3.99	142.86	13.18	8.81	6
LMH	260.01	35:56:1	0.63	35	5.35	3.62	132.40	10.62	10.97	6.5
TTS	238.36	20:20:1	1.00	20	11.28	4.11	183.67	15.01	11.40	6.8
DGS	246.54	22:23:1	0.94	22	10.49	3.69	177.12	12.25	12.67	6.45
YQS	261.78	79:97:1	0.82	79	−14.43	3.86	152.11	12.41	−7.84	2.3
EGK	294.86	17:18:1	0.96	17	12.07	3.77	179.33	12.84	15.95	7.75
FGT	299.18	14:16:1	0.85	14	13.65	3.75	159.02	11.84	19.07	7.6
FKY	271.52	13:21:1	0.62	13	14.05	3.60	132.55	10.46	19.88	7.8
SKK	172.98	12:23:1	0.50	12	14.44	3.13	138.02	3.48	20.88	8.45
KSC	270.69	20:32:1	0.61	20	11.28	3.52	133.21	9.77	17.67	8.15

α–the concentration ratio of caffeine, EGCG, and Que-rut; β–the concentration ratio of caffeine and EGCG; γ–the concentration ratio of caffeine and Que-rut.

4. Conclusions

This study developed a quantification curve to evaluate BAIPI in green tea, based on its unique flavor profile. Caffeine, EGCG, and Que-rut were identified as primary contributors to BAIPI, which were also subsequently employed to develop the quantification curve. The utilization of 2-AFC test enhanced the assessment reliability of subjects in this research, with all the fit curves conforming to the Weber–Fechner law. The slope and X-intercept of the fit curve were exponentially related to the concentration ratio of caffeine and EGCG (n). The initial BAIPI values of the fit curve were linearly associated with the concentration ratio of caffeine and Que-rut (q). Thus, BAIPI values were calculated by inputting concentrations of the three key compounds into the BAIPI quantification curve. Validation showed strong correlation with direct assessment. The R^2 and SEE of the correlation analysis were about 0.94 and 1.51, respectively. This work advances the objective assessment of tea sensory properties while offering practical tools for industry applications. However, further research integrating biochemical, genetic, and larger-scale sensory data will strengthen the robustness of this approach. These findings pave the way for more precise flavor profiling, quality control, and consumer-driven product design in the tea and broader beverage sector.

Author Contributions: Conceptualization, S.L. and Z.W.; methodology, S.L.; software, D.D.; validation, S.C.; formal analysis, D.D.; investigation, S.C.; resources, D.D.; data curation, S.L.; writing—original draft preparation, S.L.; writing—review and editing, S.L.; visualization, Z.W.; supervision, Z.W.; project administration, Z.W.; funding acquisition, Z.W. All authors have read and agreed to the published version of the manuscript.

Funding: The work was funded by the National Natural Science Foundation of China [grant number 31972200].

Institutional Review Board Statement: Ethical approval for the involvement of human subjects in this study was granted by the Medical Ethics Committee in School of Medicine of Zhejiang University, Reference number 2019-046, dtd 3 April 2019. All subjects signed a consent form to participate in the sensory and consumer tests.

Informed Consent Statement: Informed consent was obtained from all subjects involved in the study. Written informed consent has been obtained from the patients to publish this paper.

Data Availability Statement: Data will be made available on request.

Acknowledgments: The authors are grateful to the financial support from the National Natural Science Foundation of China (NSFC, 31972200) and technical support from Zhejiang University.

Conflicts of Interest: All authors declared that there was no conflicts of interest.

References

1. Wang, J.Q.; Fu, Y.Q.; Chen, J.X.; Wang, F.; Feng, Z.H.; Yin, J.F.; Zeng, L.; Xu, Y.Q. Effects of baking treatment on the sensory quality and physicochemical properties of green tea with different processing methods. *Food Chem.* **2022**, *380*, 132217. [CrossRef] [PubMed]
2. Ye, J.-H.; Ye, Y.; Yin, J.-F.; Jin, J.; Liang, Y.-R.; Liu, R.-Y.; Tang, P.; Xu, Y.-Q. Bitterness and astringency of tea leaves and products: Formation mechanism and reducing strategies. *Trends Food Sci. Technol.* **2022**, *123*, 130–143. [CrossRef]
3. Lu, L.; Wang, L.; Liu, R.Y.; Zhang, Y.B.; Zheng, X.Q.; Lu, J.L.; Wang, X.C.; Ye, J.H. An efficient artificial intelligence algorithm for predicting the sensory quality of green and black teas based on the key chemical indices. *Food Chem.* **2024**, *441*, 138341. [CrossRef]
4. Romeo-Arroyo, E.; Mora, M.; Noguera-Artiaga, L.; Vazquez-Araujo, L. Tea pairings: Impact of aromatic congruence on acceptance and sweetness perception. *Curr. Res. Food Sci.* **2023**, *6*, 100432. [CrossRef]
5. Chong, P.H.; Chen, J.; Yin, D.; Qin, L. Tea compound-saliva interactions and their correlations with sweet aftertaste. *Npj Sci. Food* **2022**, *6*, 13. [CrossRef]
6. Nolden, A.A.; Feeney, E.L. Genetic Differences in Taste Receptors: Implications for the Food Industry. *Annu. Rev. Food Sci. Technol.* **2020**, *11*, 183–204. [CrossRef]

7. Yin, J.F.; Zhang, Y.N.; Du, Q.Z.; Chen, J.X.; Yuan, H.B.; Xu, Y.Q. Effect of Ca^{2+} concentration on the tastes from the main chemicals in green tea infusions. *Food Res. Int.* **2014**, *62*, 941–946. [CrossRef]
8. Zhang, Y.N.; Yin, J.F.; Chen, J.X.; Wang, F.; Du, Q.Z.; Jiang, Y.W.; Xu, Y.Q. Improving the sweet aftertaste of green tea infusion with tannase. *Food Chem.* **2016**, *192*, 470–476. [CrossRef]
9. Chong, P.H.; Chen, J.; Yin, D.; Upadhyay, R.; Mo, L.; Han, L. "Oral" tribology study on saliva-tea compound mixtures: Correlation between sweet aftertaste (Huigan) perception and friction coefficient. *Food Res. Int.* **2019**, *125*, 108642. [CrossRef]
10. Jiang, Y.; Gong, N.N.; Matsunami, H. Astringency: A More Stringent Definition. *Chem. Senses* **2014**, *39*, 467–469. [CrossRef]
11. Lyu, J.; Fu, J.; Chen, S.; Xu, Y.; Nie, Y.; Tang, K. Impact of tannins on intraoral aroma release and retronasal perception, including detection thresholds and temporal perception by taste, in model wines. *Food Chem.* **2022**, *375*, 131890. [CrossRef] [PubMed]
12. Zeng, Y.; Liang, J.H.; Zhang, J.Y.; Chen, W.; Hu, D.; Xia, H.L.; Ma, C.Y.; Qiao, X.Y. Improvement of the sensory characteristics of Dancong tea using a dry-heating post-treatment approach. *LWT—Food Sci. Technol.* **2023**, *185*, 115118. [CrossRef]
13. De Toffoli, A.; Spinelli, S.; Monteleone, E.; Arena, E.; Di Monaco, R.; Endrizzi, I.; Toschi, T.G.; Laureati, M.; Napolitano, F.; Torri, L.; et al. Influences of Psychological Traits and PROP Taster Status on Familiarity with and Choice of Phenol-Rich Foods and Beverages. *Nutrients* **2019**, *11*, 1329. [CrossRef] [PubMed]
14. Mao, Y.Z.; Tian, S.Y.; Qin, Y.M.; Han, J.Z. A new sensory sweetness definition and sweetness conversion method of five natural sugars, based on the Weber-Fechner Law. *Food Chem.* **2019**, *281*, 78–84. [CrossRef]
15. Hayashi, N.; Ujihara, T.; Chen, R.; Irie, K.; Ikezaki, H. Objective evaluation methods for the bitter and astringent taste intensities of black and oolong teas by a taste sensor. *Food Res. Int.* **2013**, *53*, 816–821. [CrossRef]
16. Ye, Q.Q.; Chen, G.S.; Pan, W.; Cao, Q.Q.; Zeng, L.; Yin, J.F.; Xu, Y.Q. A predictive model for astringency based on in vitro interactions between salivary proteins and (−)-Epigallocatechin gallate. *Food Chem.* **2021**, *340*, 127845. [CrossRef]
17. Hayashi, N.; Chen, R.; Hiraoka, M.; Ujihara, T.; Ikezaki, H. β-Cyclodextrin/Surface Plasmon Resonance Detection System for Sensing Bitter-Astringent Taste Intensity of Green Tea Catechins. *J. Agric. Food Chem.* **2010**, *58*, 8351–8356. [CrossRef]
18. Li, S.; Du, D.; Wang, J.; Wei, Z. Application progress of intelligent flavor sensing system in the production process of fermented foods based on the flavor properties. *Crit. Rev. Food Sci. Nutr.* **2022**, *64*, 3764–3793. [CrossRef]
19. Zhang, J.; Zhao, X.; Li, L.; Chen, W.; Zhao, Q.; Su, G.; Zhao, M. Application of electronic tongue in umami detection and soy sauce refining process. *Food Chem. X* **2023**, *18*, 100652. [CrossRef]
20. Portugal, R.D.; Svaiter, B.F. Weber-Fechner Law and the Optimality of the Logarithmic Scale. *Minds Mach.* **2011**, *21*, 73–81. [CrossRef]
21. Mao, Y.; Tian, S.; Qin, Y.; Cheng, S. An optimized organic acid human sensory sourness analysis method. *J. Sci. Food Agric.* **2021**, *101*, 5880–5887. [CrossRef] [PubMed]
22. Mao, Y.Z.; Tian, S.Y.; Qin, Y.M.; Chen, S.W. Sensory sweetness and sourness interactive response of sucrose-citric acid mixture based on synergy and antagonism. *Npj Sci. Food* **2022**, *6*, 33. [CrossRef] [PubMed]
23. Wang, Y.; Wan, S.; Pan, S.; Luan, P.; Cen, X.; Sun, G.; Feng, Y.; Zhu, M. A quantitative equation for umami evaluation of food and condiments based on the Weber-Fechner law. *Food Qual. Prefer.* **2025**, *123*, 105347. [CrossRef]
24. Scharbert, S.; Hofmann, T. Molecular definition of black tea taste by means of quantitative studies, taste reconstitution, and omission experiments. *J. Agric. Food Chem.* **2005**, *53*, 5377–5384. [CrossRef]
25. Kishi, M.; Sadachi, H.; Nakamura, J.; Tonoike, M. Functional magnetic resonance imaging investigation of brain regions associated with astringency. *Neurosci. Res.* **2017**, *122*, 9–16. [CrossRef]
26. Huang, Y.L.; Vivian, R.M.; Goh, A.; Quan, S.; Sakumoto, S.; Yun, H.; Huey, K.; Sun, J.C.; Lassabliere, B.; Yu, B. Effect of three milling processes (cyclone-, bead- and stone-millings) on the quality of matcha: Physical properties, taste and aroma. *Food Chem.* **2022**, *372*, 131202. [CrossRef]
27. Liu, Y.; Luo, L.H.; Liao, C.X.; Chen, L.; Wang, J.; Zeng, L. Effects of brewing conditions on the phytochemical composition, sensory qualities and antioxidant activity of green tea infusion: A study using response surface methodology. *Food Chem.* **2018**, *269*, 24–34. [CrossRef]
28. Yu, J.Y.; Liu, Y.; Zhang, S.R.; Luo, L.Y.; Zeng, L. Effect of brewing conditions on phytochemicals and sensory profiles of black tea infusions: A primary study on the effects of geraniol and β-ionone on taste perception of black tea infusions. *Food Chem.* **2021**, *354*, 129504. [CrossRef]
29. Zhang, L.; Cao, Q.Q.; Granato, D.; Xu, Y.Q.; Ho, C.T. Association between chemistry and taste of tea: A review. *Trends Food Sci. Technol.* **2020**, *101*, 139–149. [CrossRef]
30. Daniel Estevez-Lopez, R.; Garcia-Gomez, B.; Lourdes Vazquez-Oderiz, M.; Munoz Ferreiro, N.; Angeles Romero-Rodriguez, M. Influence of bread shape on the sensory characteristics of Galician breads: Development of lexicon, efficacy control of the trained panel and establishment of a sensory profile. *LWT—Food Sci. Technol.* **2021**, *135*, 110024.
31. *ISO 8586*; Sensory Analysis. General Guidelines for the Selection, Training and Monitoring of Selected Assessors and Expert Sensory Assessors. International Organization for Standardization: Geneva, Switzerland, 2012.

32. *ISO 5495*; Sensory Analysis. Methodology. Paired Comparison Test. International Organization for Standardization: Geneva, Switzerland, 2005.
33. Kim, H.O.; Li-Chan, E.C.Y. Quantitative structure-activity relationship study of bitter peptides. *J. Agric. Food Chem.* **2006**, *54*, 10102–10111. [CrossRef] [PubMed]
34. Feng, B.L.; Ren, H.B.; Duan, J.H.; Zhang, H.S.; Wen, C.H.; Bai, X.S.; Gao, F.; Wang, Y.T. Molecular recognition and threshold prediction model of bitterness in natural compounds. *Sci. Technol. Food Ind.* **2022**, *43*, 24–32.
35. Shitandi, A.A.; Muigai Ngure, F.; Mahungu, S.M. Chapter 16—Tea Processing and its Impact on Catechins, Theaflavin and Thearubigin Formation. In *Tea in Health and Disease Prevention*; Preedy, V.R., Ed.; Academic Press: Cambridge, MA, USA, 2013; pp. 193–205.
36. Narukawa, M.; Kimata, H.; Noga, C.; Watanabe, T. Taste characterisation of green tea catechins. *Int. J. Food Sci. Technol.* **2010**, *45*, 1579–1585. [CrossRef]
37. Rong, W.; Zhou, W.; Wen, R.A.H. Kinetic study of the thermal stability of tea catechins in aqueous systems using a microwave reactor. *J. Agric. Food Chem.* **2006**, *54*, 5924–5932.
38. Ananingsih, V.K.; Sharma, A.; Zhou, W. Green tea catechins during food processing and storage: A review on stability and detection. *Food Res. Int.* **2013**, *50*, 469–479. [CrossRef]
39. Norwich, K.H.; Wong, W. Unification of psychophysical phenomena: The complete form of Fechner's law. *Percept. Psychophys.* **1997**, *59*, 929–940. [CrossRef]
40. Ishizu, T.; Tsutsumi, H.; Sato, T. Mechanism of Creaming Down Based on Chemical Characterization of a Complex of Caffeine and Tea Catechins. *Chem. Pharm. Bull.* **2016**, *64*, 676–686. [CrossRef]
41. Zhou, Z.; Ou, M.; Shen, W.; Jin, W.; Yang, G.; Huang, W.; Guo, C. Caffeine weakens the astringency of epigallocatechin gallate by inhibiting its interaction with salivary proteins. *Food Chem.* **2024**, *460*, 140753. [CrossRef]
42. Li, C.X.; Ren, Y.N.; Yao, J.; Wang, Y.L.; Gao, X.L.; Li, H.; Guo, X.F.; Liu, R.X.; Li, X.L. Study on quantitative method of specific bitterness of bitter compounds based on traditional human taste panel method. *Chin. Tradit. Herb. Drugs* **2023**, *54*, 2758–2764.
43. Li, X.L.; Gui, X.J.; Liu, R.X.; Gao, X.J.; Meng, X.L.; Chen, P.J.; Kang, B.Y.; Zhang, L.; Shi, J.H. Bitterness intensity prediction of bitter compounds of traditional Chinese medicine based on an electronic tongue. *Chin. J. New Drugs* **2016**, *25*, 1307–1314.
44. Zhu, Y.W.; Zhou, X.R.; Chen, Y.P.; Liu, Z.Y.; Jiang, S.; Chen, G.L.; Liu, Y. Exploring the relationships between perceived umami intensity, umami components and electronic tongue responses in food matrices. *Food Chem.* **2022**, *368*, 130849. [CrossRef] [PubMed]

Disclaimer/Publisher's Note: The statements, opinions and data contained in all publications are solely those of the individual author(s) and contributor(s) and not of MDPI and/or the editor(s). MDPI and/or the editor(s) disclaim responsibility for any injury to people or property resulting from any ideas, methods, instructions or products referred to in the content.